# Parametric study of a Hill-type hyperelastic skeletal muscle model

**Y T Lu**[1,2*], **L Beldie**[3], **B Walker**[3], **S Richmond**[2], and **J Middleton**[2]
[1]School of Engineering, Cardiff University, Queen's Buildings, The Parade, Cardiff, Wales, UK
[2]School of Dentistry, Cardiff University, Heath Park, Cardiff, Wales, UK
[3]Ove Arup & Partners Ltd, Solihull, UK

*The manuscript was received on 18 June 2010 and was accepted after revision for publication on 8 October 2010.*

DOI: 10.1177/2041303310392632

**Abstract:** Hill's one-dimensional three-element model has often been used for formulating a three-dimensional skeletal muscle constitutive model, which generally involves several material parameters. However, only few of these parameters have physical meanings and can be experimentally determined. In this paper, a parametric study of a Hill-type hyperelastic skeletal muscle model is performed. First, the Hill-type hyperelastic skeletal muscle model is formulated, containing 13 material parameters. The values or value ranges of these parameters are discussed. The muscle model is then used to predict the behaviour of New Zealand white rabbit hind leg muscle tibialis anterior and a sensitivity study of several parameters is performed. Results show that some parameters in the muscle model can be experimentally determined, some parameters have their own value ranges and the muscle model can predict the experimental data by tuning the parameters within their value ranges. The results from the sensitivity study can help understand how some parameters influence the total muscle stress.

**Keywords:** skeletal muscle, finite element, constitutive model, parametric study, LS-DYNA UMAT

## 1 INTRODUCTION

Skeletal muscle is a soft biological tissue with the primary function of active contraction. Skeletal muscle plays an important role in the human body system and function by generating voluntary forces and facilitating body motion. Furthermore, skeletal muscle provides protection to the upright skeleton. From a biomechanical point of view, skeletal muscle exhibits a very complex mechanical behaviour which is active, incompressible, transversely isotropic, and hyperelastic. A number of mathematical skeletal muscle models have been developed over the past two decades and they can be classified as belonging to one of two categories: Hill-type [**1**] and Huxley-type [**2**] muscle models. Hill-type muscle models are phenomenologically based and consist of three elements: a parallel element (PE) in parallel with a series elastic element (SEE) and a contractile element (CE). Huxley-type models describe the muscle behaviour at the molecular level and are mainly used to understand the properties of the microscopic contractile element. In this paper, the Hill-type muscle models are studied and discussed.

Hill's three-element model has been used in studying the mechanical behaviour of different muscle tissues [**3–6**]. However, Hill's model is only one-dimensional (1D). In order to investigate the complex three-dimensional (3D) geometry and mechanical behaviour of skeletal muscle, Hill's 1D model has been extended into the 3D scope. The approach of muscle model extension, which has been employed by many researchers [**7–13**], is to add up the longitudinal stress from the muscle fibres $\boldsymbol{\sigma}_{\text{fibre}}$, the stress from the embedding matrix $\boldsymbol{\sigma}_{\text{matrix}}$ and the stress related to the incompressibility of the muscle $\boldsymbol{\sigma}_{\text{incomp}}$. Thus, the Cauchy stress $\boldsymbol{\sigma}$ produced in a 3D muscle can be expressed as

$$\boldsymbol{\sigma} = \boldsymbol{\sigma}_{\text{fibre}} + \boldsymbol{\sigma}_{\text{matrix}} + \boldsymbol{\sigma}_{\text{incomp}} \quad (1)$$

In the 3D Hill-type skeletal muscle model proposed by Kojic *et al.* [**10**], the contractile element and the

*Corresponding author: School of Engineering (Research Office), Cardiff University, Cardiff, CF24 3AA, Wales, UK.
email: Luy11@cardiff.ac.uk

series elastic element played the role of the active muscle fibre, and the parallel element played the role of the surrounding matrix which was assumed to be isotropic linear elastic. The incompressibility constraint was not taken into account. There are ten material parameters involved in Kojic *et al.*'s model. In the same year, Martins *et al.* [**11**] developed a 3D Hill-type skeletal muscle model based on the concept of fibre-reinforced composite. This was a modified form of the constitutive equation proposed by Humphrey and Yin [**14**]. The material parameters in Martins *et al.*'s model were reduced to 4. However, a strain-like quantity $\xi^{CE}$ was introduced into their model to express the stress in the CE and this quantity is difficult for the experimental determination. To avoid using $\xi^{CE}$, Martins *et al.* [**12**] introduced the multiplicative split of the fibre stretch into a contractile stretch followed by an elastic stretch and through this method, the number of material parameters was controlled at 5. Most recently, Tang *et al.*'s [**13**] developed a 3D finite element muscle model which was able to simulate active and passive nonlinear mechanical behaviour of skeletal muscle during lengthening or shortening under either quasi-static or dynamic condition. This model is comprehensive, but there are 11 material parameters involved and few of them are well understood.

In this paper, the parametric study of a Hill-type hyperelastic muscle model is performed. In this model, the muscle is modelled as an active, quasi-incompressible, transversely isotropic and hyperelastic solid. There are 13 material parameters in the developed muscle model. The values or value ranges of these parameters are investigated. A test is then performed to investigate if the model can be used to predict some experimental data by tuning the parameters within their value ranges. The results from the sensitivity study of some material parameters are also included in the paper.

## 2 SKELETAL MUSCLE CONSTITUTIVE MODEL

The muscle constitutive relation is derived through the strain energy approach and the framework of this relation is adopted from Tang *et al.*'s work [**13**]. However, in order to reduce the parameter inputs, the muscle force-length function in Tang *et al.*'s model is replaced with a smooth quadratic function proposed by Blemker *et al.* [**15**]. Furthermore, in order to control the muscle activation behavior, Tang *et al.*'s muscle activation function is replaced by an exponential function proposed by Meier and Blickhan [**16**]. The skeletal muscle model is summarized below.

The muscle is regarded as a fibre-reinforced composite comprising a ground substance matrix and the muscle fibres, where the muscle fibres are modeled using the Hill's three-element model (Fig. 1).

The strain energy in the muscle is given by

$$U = U_I\left(\bar{I}_1^C\right) + U_{\mathrm{f}}\left(\bar{\lambda}_{\mathrm{f}}, \lambda_{\mathrm{s}}\right) + U_J(J) \tag{2}$$

where

$$U_I\left(\bar{I}_1^C\right) = c\left\{\exp\left[b\left(\bar{I}_1^C - 3\right)\right] - 1\right\} \tag{3}$$

is the strain energy stored in the isotropic matrix

$$\mathrm{U_f}(\bar{\lambda}_{\mathrm{f}}, \lambda_{\mathrm{s}}) = \int_1^{\bar{\lambda}_{\mathrm{f}}} [\sigma_{\mathrm{s}}(\lambda, \lambda_{\mathrm{s}}) + \sigma_{\mathrm{p}}(\lambda)] d\lambda \tag{4}$$

is the strain energy stored in the muscle fibres and

$$U_J(J) = \frac{1}{D}(J-1)^2 \tag{5}$$

is the strain energy associated with the volume change.

In these definitions, $\bar{I}_1^C$ is the first invariant of the right Cauchy–Green strain tensor with the volume change eliminated, $b$ and $c$ are material parameters, $\bar{\lambda}_{\mathrm{f}}$ is the modified fibre stretch ratio, $\lambda_{\mathrm{s}}$ is the stretch ratio in the series elastic element (SEE), $\lambda$ is the fibre stretch ratio, $\sigma_{\mathrm{s}}(\lambda, \lambda_{\mathrm{s}})$ is the stress produced in SEE, $\sigma_{\mathrm{p}}(\lambda)$ is the stress produced in the parallel element (PE), $J$ is the Jacobian of the deformation gradient and $D$ is the compressibility constant.

Based on Pinto and Fung's experiment on the papillary muscle of a rabbit heart, Fung proposed a recurrence relation to express the stress produced in the SEE [**17**]

$${}^{t+\Delta t}\sigma_{\mathrm{s}} = \mathrm{e}^{\alpha \Delta \lambda_{\mathrm{s}}}\left({}^{t}\sigma_{\mathrm{s}} + \beta\right) - \beta \tag{6}$$

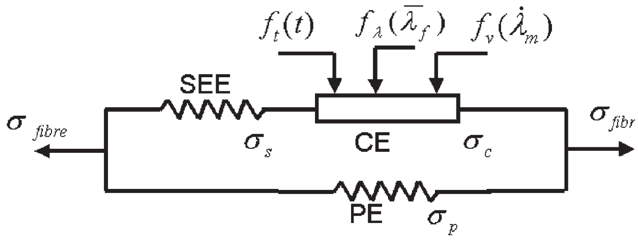


**Fig. 1** Hill's three-element muscle model

with

$$ {}^{t}\sigma_{\mathrm{s}} = \beta\left[\mathrm{e}^{\alpha({}^{t}\lambda_{\mathrm{s}}-1)} - 1\right] \tag{7}$$

where $\alpha$ and $\beta$ are material constants.

The stress produced in the CE is given by

$$ {}^{\mathrm{t}+\Delta\mathrm{t}}\sigma_c = \sigma_0 \cdot f_t(t+\Delta t)\cdot f_\lambda(\bar{\lambda}_f)\cdot f_v(\dot{\lambda}_m) \tag{8}$$

where

$$ f_{\mathrm{t}}(t) = \begin{cases} n_1, & \text{if} \quad t < t_0 \\ n_1 + (n_2 - n_1)\cdot h_{\mathrm{t}}(t, t_0), & \text{if} \quad t_0 < t < t_1 \\ n_1 + (n_2 - n_1)\cdot h_{\mathrm{t}}(t_1, t_0) & \\ \quad - [(n_2 - n_1)\cdot h_t(t_1, t_0)]\cdot h_{\mathrm{t}}(t, t_1), & \text{if} \quad t > t_1 \end{cases} \tag{9}$$

with

$$ h_{\mathrm{t}}(t_{\mathrm{i}}, t_{\mathrm{b}}) = \{1 - \exp[-S\cdot(t_{\mathrm{i}} - t_{\mathrm{b}})]\} \tag{10}$$

is the muscle activation function;

$$ f_\lambda\left({}^{t}\bar{\lambda}_{\mathrm{f}}\right) = \begin{cases} 0, & \text{if} \quad {}^{t}\bar{\lambda}_{\mathrm{f}}/\lambda_{\mathrm{opt}} < 0.4 \\ 9\left({}^{t}\bar{\lambda}_{\mathrm{f}}/\lambda_{\mathrm{opt}} - 0.4\right)^2, & \text{if} \quad 0.4 \leqslant {}^{t}\bar{\lambda}_{\mathrm{f}}/\lambda_{\mathrm{opt}} < 0.6 \\ 1 - 4\left(1 - {}^{t}\bar{\lambda}_{\mathrm{f}}/\lambda_{\mathrm{opt}}\right)^2, & \text{if} \quad 0.6 \leqslant {}^{t}\bar{\lambda}_{\mathrm{f}}/\lambda_{\mathrm{opt}} < 1.4 \\ 9\left({}^{t}\bar{\lambda}_{\mathrm{f}}/\lambda_{\mathrm{opt}} - 1.6\right)^2, & \text{if} \quad 1.4 \leqslant {}^{t}\bar{\lambda}_{\mathrm{f}}/\lambda_{\mathrm{opt}} < 1.6 \\ 0, & \text{if} \quad {}^{t}\bar{\lambda}_{\mathrm{f}}/\lambda_{\mathrm{opt}} \geq 1.6 \end{cases} \tag{11}$$

is the muscle stress-stretch function and

$$ f_{\mathrm{v}}\left(\dot{\lambda}_{\mathrm{m}}\right) = \begin{cases} \dfrac{1 - \dot{\lambda}_{\mathrm{m}}\big/\dot{\lambda}_{\mathrm{m}}^{\min}}{1 + k_{\mathrm{c}}\dot{\lambda}_{\mathrm{m}}\big/\dot{\lambda}_{\mathrm{m}}^{\min}}, & \text{if} \quad \dot{\lambda}_m \leqslant 0 \\ d - (d-1)\dfrac{1 + \dot{\lambda}_{\mathrm{m}}\big/\dot{\lambda}_{\mathrm{m}}^{\min}}{1 - k_{\mathrm{c}}k_{\mathrm{e}}\dot{\lambda}_{\mathrm{m}}\big/\dot{\lambda}_{\mathrm{m}}^{\min}}, & \text{if} \quad \dot{\lambda}_m > 0 \end{cases} \tag{12}$$

is the muscle stress-velocity function.

In these definitions, $\sigma_0$ is the maximum isometric stress, $n_1$ is the muscle activation level before and after the activation, $n_2$ is the muscle activation level during the activation, $t_0$ is the muscle activation time, $t_1$ is the muscle deactivation time, $S$ is the exponential factor, $\lambda_{\mathrm{opt}}$ is the optimal fibre stretch, $k_{\mathrm{c}}$ and $k_{\mathrm{e}}$ are the shape parameters of the hyperbolic curves, $d$ is the offset of the eccentric function, $\dot{\lambda}_{\mathrm{m}}$ is the stretch rate in the CE, and $\dot{\lambda}_{\mathrm{m}}^{\min}$ is the minimum stretch rate.

Equation (6) contains one unknown, namely $\Delta\lambda_{\mathrm{s}}$, and this can be solved by setting up a non-linear equation utilising the stresses relationship between the CE and the SEE [**13**], i.e. at any time, ${}^{t+\Delta t}\sigma_{\mathrm{s}} = {}^{t+\Delta t}\sigma_{\mathrm{c}}$. Further using equations (6) and (8), the following non-linear equation is obtained

$$ f(\Delta\lambda_{\mathrm{s}}) = (\alpha_2 + \alpha_3\Delta\lambda_{\mathrm{s}})\mathrm{e}^{\alpha\Delta\lambda_{\mathrm{s}}} - \alpha_4\Delta\lambda_{\mathrm{s}} - \alpha_5 = 0 \tag{13}$$

where in case of muscle shortening

$$ \alpha_2 = \left({}^{t}\sigma_{\mathrm{s}} + \beta\right)\left(1 + \frac{k_{\mathrm{c}}\cdot\alpha_1}{\dot{\lambda}_{\mathrm{m}}^{\min}\cdot\Delta t}\right) \tag{14}$$

$$ \alpha_3 = -\left({}^{t}\sigma_{\mathrm{s}} + \beta\right)\frac{k\cdot k_{\mathrm{c}}}{\dot{\lambda}_{\mathrm{m}}^{\min}\cdot\Delta t} \tag{15}$$

$$ \alpha_4 = -\frac{\beta\cdot k_c - f_\lambda({}^{t}\bar{\lambda}_f)\cdot f_{\mathrm{t}}(t+\Delta t)}{\dot{\lambda}_m^{min}\cdot\Delta t}k \tag{16}$$

$$ \alpha_5 = \beta + f_\lambda\left({}^{t}\bar{\lambda}_{\mathrm{f}}\right)\cdot f_{\mathrm{t}}(t+\Delta t) - \frac{f_\lambda\left({}^{t}\bar{\lambda}_{\mathrm{f}}\right)\cdot f_{\mathrm{t}}(t+\Delta t) - \beta\cdot k_{\mathrm{c}}}{\dot{\lambda}_{\mathrm{m}}^{\min}\cdot\Delta t}\alpha_1 \tag{17}$$

and in case of muscle lengthening

$$ \alpha_2 = \left({}^{t}\sigma_{\mathrm{s}} + \beta\right)\left(1 - \frac{k_{\mathrm{e}}\cdot k_{\mathrm{c}}\cdot\alpha_1}{\dot{\lambda}_{\mathrm{m}}^{\min}\cdot\Delta t}\right) \tag{18}$$

$$ \alpha_3 = \left({}^{t}\sigma_{\mathrm{s}} + \beta\right)\frac{k\cdot k_{\mathrm{e}}\cdot k_{\mathrm{c}}}{\dot{\lambda}_{\mathrm{m}}^{\min}\cdot\Delta t} \tag{19}$$

$$ \alpha_4 = \frac{\beta\cdot k_{\mathrm{e}}\cdot k_{\mathrm{c}} + f_\lambda\left({}^{t}\bar{\lambda}_{\mathrm{f}}\right)\cdot f_{\mathrm{t}}(t+\Delta t)\cdot(d\cdot k_{\mathrm{e}}\cdot k_{\mathrm{c}} + d - 1)}{\dot{\lambda}_{\mathrm{m}}^{\min}\cdot\Delta t}k \tag{20}$$

$$ \alpha_5 = \beta + {}^{t}f_\lambda\left(\bar{\lambda}_{\mathrm{f}}\right)\cdot f_{\mathrm{t}}(t+\Delta t) - \frac{f_\lambda\left({}^{t}\bar{\lambda}_{\mathrm{f}}\right)\cdot f_{\mathrm{t}}(t+\Delta t)\cdot(1 - d - d\cdot k_{\mathrm{e}}\cdot k_{\mathrm{c}}) - \beta\cdot k_{\mathrm{e}}\cdot k_{\mathrm{c}}}{\dot{\lambda}_{\mathrm{m}}^{\min}\cdot\Delta t}\alpha_1 \tag{21}$$

In equations (14), (17), (18), and (21), $\alpha_1 = (1+k)^{t+\Delta t}\bar{\lambda}_{\mathrm{f}} - {}^{t}\lambda_{\mathrm{m}} - k^{t}\lambda_{\mathrm{s}}$, where $k$ is the ratio of the length of contractile element to that of series elastic element and is normally set as 0.3.

The stress in the PE can be expressed as

$$^{t+\Delta t}\sigma_{\mathrm{p}} = \sigma_0 f_{\mathrm{PE}}\left({}^{t+\Delta t}\bar{\lambda}_{\mathrm{f}}\right) \tag{22}$$

with

$$f_{\mathrm{PE}}\left({}^{t+\Delta t}\bar{\lambda}_{\mathrm{f}}\right) = \begin{cases} A\cdot\left({}^{t+\Delta t}\bar{\lambda}_{\mathrm{f}}-1\right)^2, & \text{if } {}^{t+\Delta t}\bar{\lambda}_{\mathrm{f}} > 1 \\ 0, & \text{otherwise} \end{cases} \tag{23}$$

where $A$ is a material parameter.

Using equations (4), (6), and (22), the strain energy produced in the muscle fibres can now be obtained. Then, the second Piola–Kirchhoff stress tensor $\mathbf{S}$ can be obtained from the strain energy function (2) [**18**]

$$\mathbf{S} = \frac{\partial U}{\partial \mathbf{E}} = U'_I\left(2J^{-2/3}\mathbf{I} - \frac{2}{3}\bar{I}_1^C\mathbf{C}^{-1}\right) + U'_{\mathrm{f}}\left(J^{-2/3}\bar{\lambda}_{\mathrm{f}}^{-1}(\mathbf{A}\otimes\mathbf{A}) - \frac{1}{3}\bar{\lambda}_{\mathrm{f}}\mathbf{C}^{-1}\right) + JU'_J\mathbf{C}^{-1} \tag{24}$$

where

$$U'_I = \frac{\partial U_I}{\partial \bar{I}_1^C} = bc\exp\left[b\left(\bar{I}_1^C - 3\right)\right] \tag{25}$$

$$U'_f(\bar{\lambda}_f, \lambda_s) = U'_{PE}(\bar{\lambda}_f) + U'_{SEE}(\bar{\lambda}_f, \lambda_s) \tag{26}$$

$$U'_J = \frac{\partial U_J}{\partial J} = \frac{2}{D}(J-1) \tag{27}$$

and

$$U'_{\mathrm{PE}}\left(\bar{\lambda}_{\mathrm{f}}\right) = \sigma_0\begin{cases} 4\left(\bar{\lambda}_{\mathrm{f}}-1\right)^2, & \text{if } \bar{\lambda}_{\mathrm{f}} > 1 \\ 0, & \text{otherwise} \end{cases} \tag{28}$$

$$U'_{\mathrm{SEE}}\left(\bar{\lambda}_{\mathrm{f}}, \lambda_{\mathrm{s}}\right) = \beta\cdot\left[\mathrm{e}^{\alpha(\lambda_{\mathrm{s}}-1)} - 1\right] \tag{29}$$

In equation (24), $\mathbf{E}$ is the Green strain, $\mathbf{I}$ is the second-order unit tensor, $\mathbf{C}$ is the right Cauchy–Green tensor and $\mathbf{A}$ is the initial muscle fibre direction.

The Cauchy stress $\boldsymbol{\sigma}$ is defined by the push-forward of $\mathbf{S}$ by the deformation $\varphi$ [**19**]

$$\boldsymbol{\sigma} := \frac{1}{J}\phi(\mathbf{S}) = \frac{1}{J}\left[U'_I\left(2\bar{\mathbf{B}} - \frac{2}{3}\bar{I}_1^C\mathbf{I}\right) + U'_{\mathrm{f}}\left(\bar{\lambda}_{\mathrm{f}}(\mathbf{a}\otimes\mathbf{a}) - \frac{1}{3}\bar{\lambda}_{\mathrm{f}}\mathbf{I}\right)\right] + U'_J\mathbf{I} \tag{30}$$

where, $\bar{\mathbf{B}}$ is the left Cauchy–Green tensor and $\mathbf{a}$ is the deformed fibre direction.

## 3 PARAMETRIC STUDY OF THE SKELETAL MUSCLE MODEL

The muscle model described in section 2 is active, quasi-incompressible, transversely isotropic, and hyperelastic. The general framework for the finite element implementation of this kind of material has been described in Weiss *et al.*'s work [**20**]. In this paper, the developed model was implemented into LS-DYNA [**21**] by means of user-defined material (UMAT) subroutines. There are 13 material parameters in the muscle model, as listed in Table 1.

Parameters $b$ and $c$ are used to characterize the stress produced in the isotropic matrix and they first appeared in an exponential form expression proposed by Humphrey and Yin [**14**]. In their work, the values of $b$ and $c$ were determined in a least-squared sense from the experimental data and it was found that the best-fit material parameters varied with the experimental protocol. In this paper, the data set $b = 23.46$ and $c = 379.0$ Pa is chosen from Humphrey and Yin's best-fit data, as it was also used in the study by Martins *et al.* [**12**, **22**].

To determine the stress in the SEE, Pinto and Fung [**23**] performed experiments on the papillary muscle of a rabbit heart and it was found that the derivative of stress with respect to strain is a linearly increasing function of the stress (Fig. 2). They proposed the following equation to express the experimental result:

$$\frac{\mathrm{d}\sigma_{\mathrm{s}}}{\mathrm{d}\lambda} = \alpha(\sigma_{\mathrm{s}} + \beta) \tag{31}$$

It can be seen that $\alpha$ is the slope of the straight line and is approximate 10.0. It can be also worked out

**Table 1** Material parameters

| Stress in the matrix | | Stress in SEE | | Stress in PE | | Stress in CE | | | | | | Compressibility constant |
|---|---|---|---|---|---|---|---|---|---|---|---|---|
| | | | | | | $f_{\mathrm{t}}(t)$ | $f_{\mathrm{v}}(\dot{\lambda}_{\mathrm{m}})$ | | | | $f_{\lambda}(\bar{\lambda})_{\mathrm{f}}$ | |
| $b$ | $c$ | $\alpha$ | $\beta$ | $A$ | $\sigma_0$ | $S$ | $k_{\mathrm{c}}$ | $k_{\mathrm{e}}$ | $d$ | $\dot{\lambda}_{\mathrm{m}}^{\min}$ | $\lambda_{\mathrm{opt}}$ | $D$ |

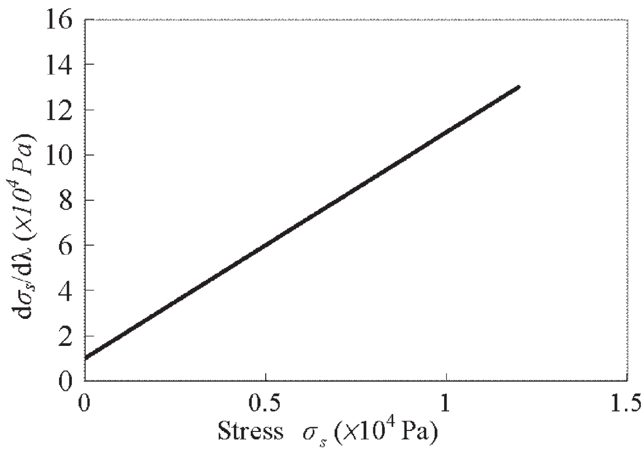


**Fig. 2** Relation between derivative of stress with respect to strain and stress

from Fig. 2 that $\alpha\beta \approx 1.0 \times 10^4$ Pa. Therefore, $\beta \approx 1.0 \times 10^3$ Pa. It should be noted that equation (31) can be integrated to equation (6).

Chen and Zelter [**24**] performed the tension-length experiment on frog muscle to measure the force for the passive muscle. To express the experimental tension–length curve, they subsequently proposed a quadratic function, as shown in equation (23), where the parameter $A$ was set to 4.0 to fit the experimental curve. When $A = 4.0$, the normalized force in PE versus stretch ratio curve derived from equation (23) is plotted against Chen and Zelter's experimental curve in Fig. 3. Parameter $\sigma_0$ is the maximum isometric stress and its value varies both from species to species and from subject to subject. However, it is reported that $\sigma_0$ ranges from 0.16 MPa to 1.0 MPa [**25**].

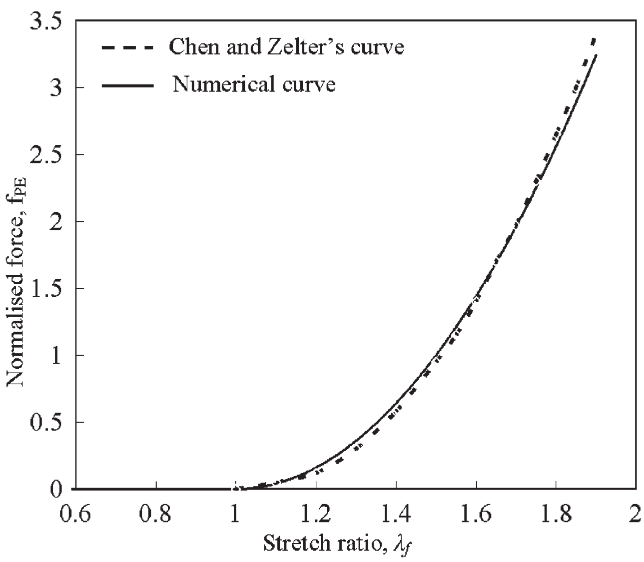


**Fig. 3** Normalized force in PE versus stretch ratio curves

There is only one parameter $S$ used to define the muscle activation function. Parameter $S$ is an exponential factor. When modelling single muscle fibres, the magnitude of $S$ is related to the rate of the chemical processes and when modelling large muscle compartments, $S$ represents the time-dependent recruitment of different motor units. Figure 4 shows the activation curves for $t_0 = 0.1$s, $t_1 = 0.4$s, $n_1 = 0.0$, and $n_2 = 1.0$, where the solid curve is with $S = 50$ and the dotted curve is with $S = 100$. In this paper, $S$ is set as 50.0 to mimic one case of the muscle activation [**16**].

Four parameters $k_c$, $k_e$, $d$, and $\dot{\lambda}_m^{min}$ are used to describe the muscle force–velocity relationship. It is reported that the value of $k_c$ for slow muscle fibres is 5.88 and its value for fast muscle fibres is 4.0 [**26**, **27**]. The influence of $k_c$ on the muscle force is shown in Fig. 5 (left), where $d$ is set as 1.8. The value of $k_e$ varies in the literature. In Van Leeuwen's work [**28**], it was chosen as 7.56. In Ből and Reese's work [**29**], it was 5 and in Tang *et al.*'s work [**13**], it was set to 3.14 for frog gastrocenemius muscle and 7.56 for squid tentacle. The influence of $k_e$ is shown in Fig. 5 (right), where $d$ is set as 1.8. The dimensionless constant $d$ is the offset of the function due to the eccentric movement. It is seen from equation (12) that the maximum eccentric stress at time $t + \Delta t$ is dominated by the parameter $d$. The ultimate tension that a muscle can sustain is limited from 1.1 $\sigma_0$ to 1.8 $\sigma_0$ [**25**]. Therefore, the value range for $d$ is from 1.1 to 1.8. It is reported that the minimum stretch rate $\dot{\lambda}_m^{min}$ is $-17$/s, although this cannot be reached owing to the inertia of muscle [**16**]. In this paper, the muscle inertia is not taken into account. Therefore, $\dot{\lambda}_m^{min}$ is chosen as $-17$/s. When $k_c = 5.0$, $k_e = 5.0$, $d = 1.8$, and $\dot{\lambda}_m^{min} = -17$, the force–velocity curve derived from equation (12) is plotted against McMahon's experimental force–velocity curve [**30**] in Fig. 6.

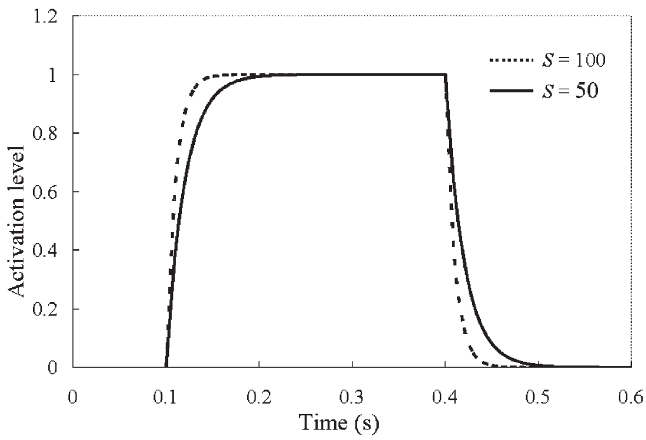


**Fig. 4** Muscle activation curves

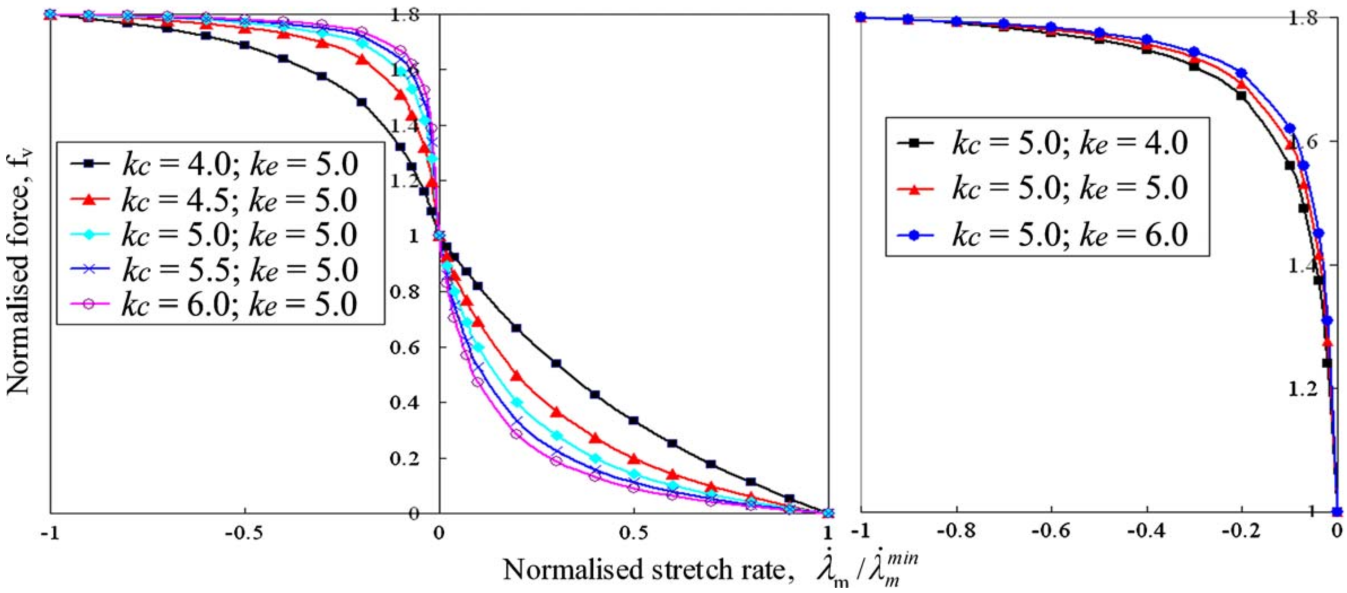


**Fig. 5** Effects of $k_c$ and $k_e$ on the normalized force versus velocity curve

In the developed muscle model, the muscle force–stretch relationship is characterized by one parameter, namely $\lambda_{opt}$. In this paper, the value of $\lambda_{opt}$ is set as 1.05 to approximate Gordon's isometric tension–length curve obtained from the experiments on a single fibre of frog skeletal muscle [**31**]. When $\lambda_{opt} = 1.05$, the curve derived from equation (11) is plotted against Gordon's experimental curve in Fig. 7.

Parameter $D$ is a compressibility constant and it can be best understood as a penalty parameter which is used to penalize the volume change. Therefore, the value of $D$ is chosen on the condition that the object volume is preserved during the deformation.

From the above analysis, it is seen that the parameters $b$, $c$, $\alpha$, $\beta$, and $A$ have been determined by best fitting with the corresponding experimental data. Parameters $\sigma_0$, $S$, $\dot{\lambda}_m^{min}$, and $\lambda_{opt}$ have their physical meanings. Parameters $k_c$, $k_e$, and $d$ are for characterising the muscle force-velocity curves. The analysis also shows that parameters $\sigma_0$, $k_c$, $k_e$, and $d$ have their own value ranges. In this paper, the investigations are performed to test if the developed muscle constitutive model can predict some experimental data by tuning the parameters within their value ranges. To do so, the experimental data from the New Zealand white rabbit hind leg muscle tibialis anterior [**32**, **33**] are used. Passive and activated elongation simulations are performed and the simulation results are compared with the experimental data.

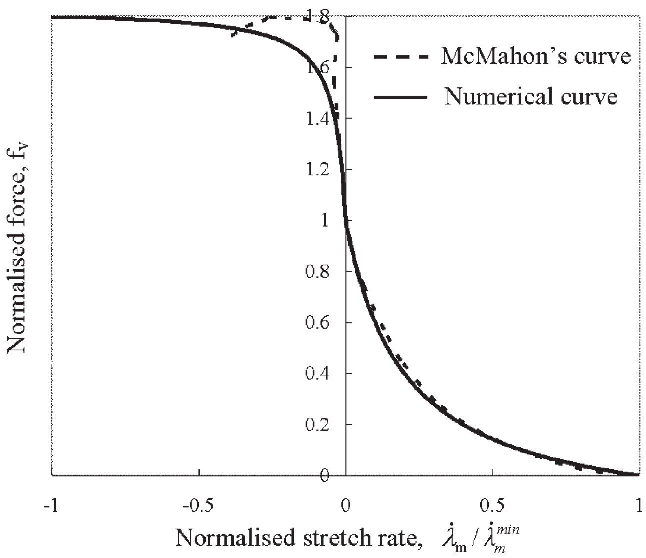


**Fig. 6** Muscle force–velocity curves

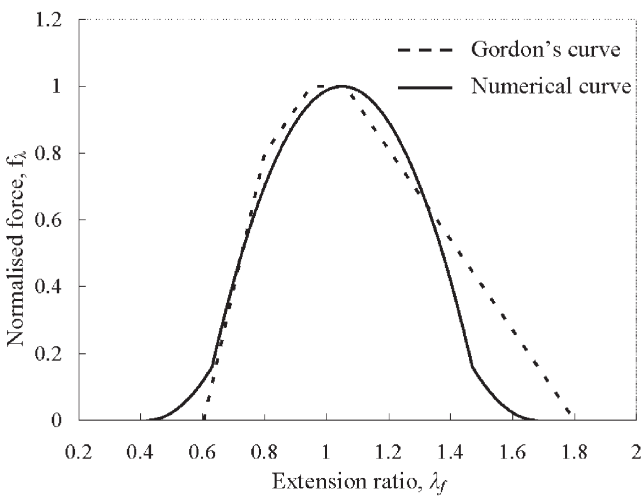


**Fig. 7** Muscle force–stretch curves

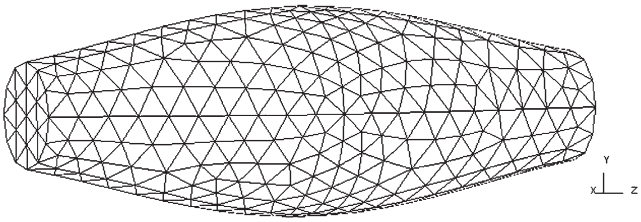

**Fig. 8** Finite element muscle model

A simple finite element muscle model shown in Fig. 8 is used for the test. Four-noded tetrahedral elements are used in the finite element FE muscle model. The length of the muscle is 5.0 cm. The diameter is 0.9 cm for the smallest cross-section and 1.75 cm for the largest cross-section. The initial direction of the parallel distributed fibre was chosen to be along longitudinal direction.

In the passive elongation simulation, one end of the muscle was fully fixed and the other end of the muscle was pulled quasi-statically at a controlled velocity of 5.0 mm/s (which is regarded as a quasi-static simulation velocity [**8**]) from its rest length, while the muscle was not activated. The activated elongation simulation was divided into two stages. In the first stage, the muscle was held constant in length while being stimulated for 0.5 s, at the end of which the muscle had reached full activation. The muscle was stimulated by inputting an activation function (Fig. 9), where $t_0 = 0.0$ s, $t_1 = 0.5$ s, $n_1 = 0.0$, and $n_2 = 1.0$. In the second stage, while one end of the muscle was still fully fixed, the other end of the muscle was released and pulled quasi-statically at a controlled velocity of 5.0 mm/s while the full activation was maintained. The engineering stress–strain curves were obtained from the two simulations and plotted against the corresponding experimental curve. The values of the parameters $\sigma_0$, $D$, $k_e$, $k_c$, and $d$ were tuned to make the numerical results fit with the experimental data. In this process, first the five parameters were tuned one by one in order to find out how they influence the stress–strain curve, and then they were tuned together until a set of fitting values were found, as listed in Table 2. Using these parameter values, the passive elongation simulation results show reasonably good agreement with the experimental data, as illustrated in Fig. 10 (left) and the results from the activated elongation are in accordance with the experimental data up to 15 per cent engineering strain, as indicated in Fig. 10 (right).

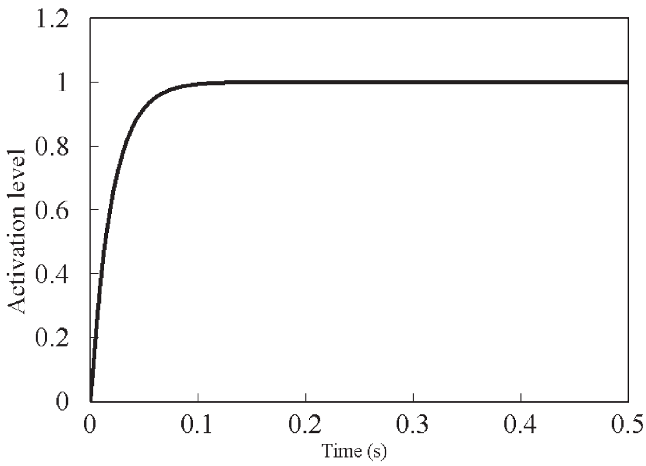


**Fig. 9** Muscle activation function

Given that some of the input parameters are effectively guessed within their values ranges, the sensitivity of these parameters needs investigating. In this paper, the sensitivity tests of $D$, $\sigma_0$, $k_c$, $k_e$, and $d$ are performed, as their values were tuned during the fitting process. In these tests, while the value of one parameter is varied, the values of the remaining 12 parameters are taken from Table 2. Since parameter $k_c$ and $d$ are used in the characterization of muscle active stress, the sensitivities of $k_c$ and $d$ are performed in the activated elongation simulation. The results from the sensitivity tests (Figs 11 and 12) show that the engineering stress increases with the

**Table 2** Material parameter values

| Description | | Parameter | Value | References |
|---|---|---|---|---|
| Stress in the matrix | | $b$ | 23.46 | Humphrey and Yin, 1987 |
| | | $c$ (Pa) | 379.0 | |
| Stress in the SEE | | $\alpha$ | 10 | Pinto and Fung, 1973 |
| | | $\beta$ (Pa) | $1.0\times10^{3}$ | |
| Stress in the PE | | $A$ | 4.0 | Chen and Zeltzer, 1992 |
| | | $\sigma_0$ ( Pa) | $7.0\times10^{5}$ | |
| Stress in the CE | $f_t(t)$ | $S(\mathrm{s}^{-1})$ | 50 | Meier and Blickhan, 2000 |
| | $f_v(\dot{\lambda}_m)$ | $k_c$ | 5 | |
| | | $k_e$ | 5 | |
| | | $d$ | 1.5 | |
| | | $\dot{\lambda}_m^{min}$ ($\mathrm{s}^{-1}$) | $-17$ | Meier and Blickhan, 2000 |
| | $f_\lambda(\bar{\lambda})_f$ | $\lambda_{opt}$ | 1.05 | Gordon, 1966 |
| Compressibility constant | | $D$ ($\mathrm{Pa}^{-1}$) | $1.0\times10^{-9}$ | |

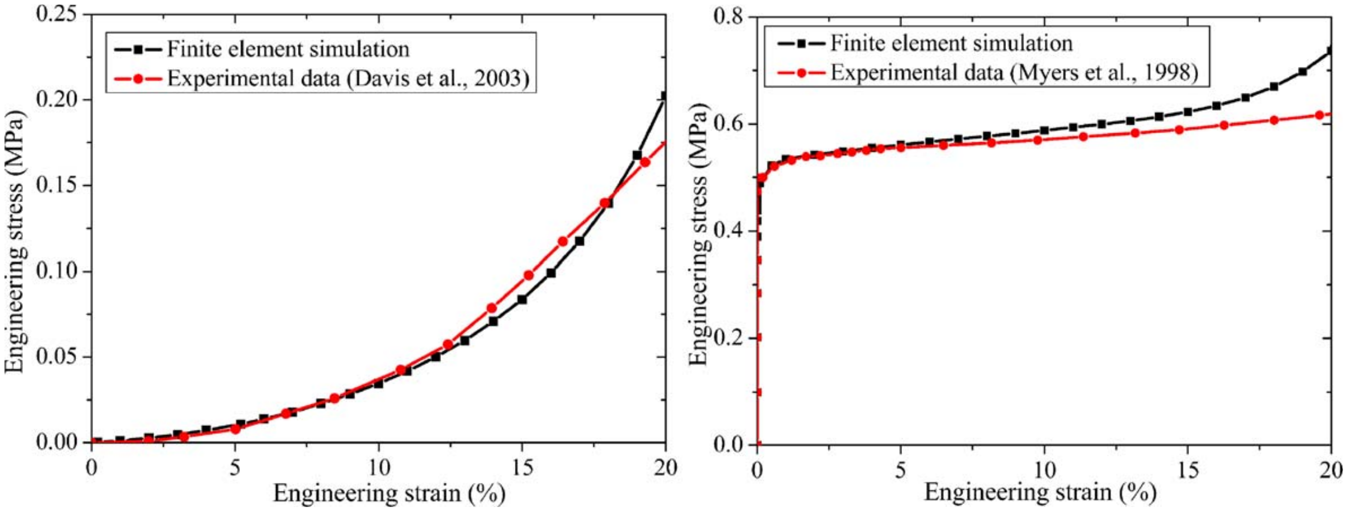


**Fig. 10** Engineering stress–strain curves compared with experimental data

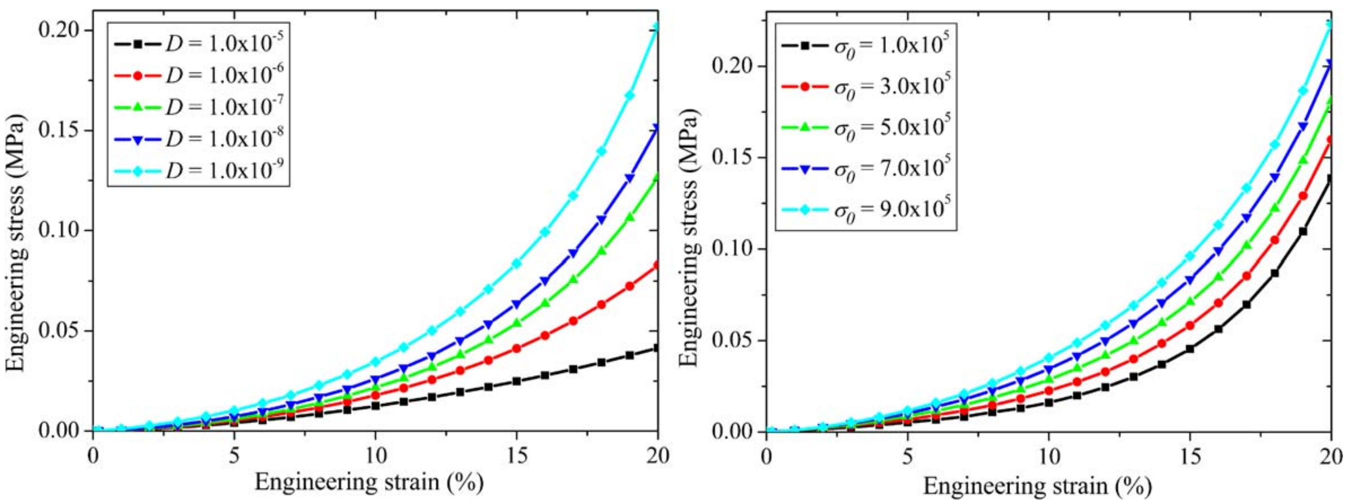


**Fig. 11** Sensitivities of parameters $D$ and $\sigma_0$ in the passive elongation simulation

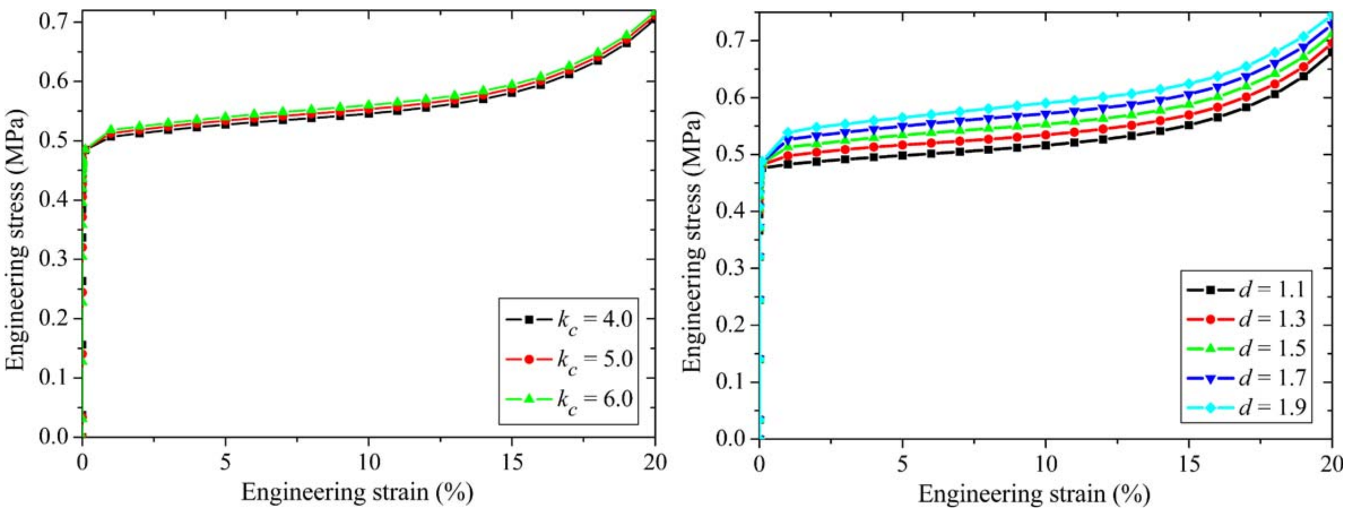


**Fig. 12** Sensitivities of parameters $k_c$ and $d$ in the activated elongation simulation

increase of $\sigma_0$, $k_c$, and $d$ and decreases with the increase of $D$. It is seen from Fig. 11 (left) that parameter $D$ has a considerable influence on the total engineering stress and so its value should be carefully chosen. In the paper, the value of $D$ is set based on the conditions that the muscle volume has been preserved and the resulting stress-strain curves fit closely to the corresponding experimental curve. Parameter $\sigma_0$ has also a considerable influence and it is seen that the relative difference between the engineering stresses at the maximal and minimal $\sigma_0$ is up to 60.7 per cent at strain 0.2. Therefore, it is crucial to choose the right value for $\sigma_0$ in the numerical simulations. Since the value variation of $\sigma_0$ depends on the muscle type, it is hoped that the value of $\sigma_0$ can be experimentally determined for individual muscle in the future. It is seen from Fig. 12 (left) that parameters $k_c$ has little influence on the muscle stress. Since parameter $k_e$ has similar effects on the muscle force-velocity curves as $k_c$ (Fig. 5), the sensitivity of $k_e$ is similar to that of $k_c$. Therefore, the sensitivity result of $k_e$ is not included here. It can be seen from Fig. 12 that parameter $d$ has a greater influence than parameter $k_c$ and $k_e$.

## 4 CONCLUSION

In this paper, a parametric study of a three-dimensional Hill-type finite element muscle model has been presented. The muscle constitutive model is based on Tang *et al.*'s work [**13**] and is able to characterize the complex mechanical behaviour of skeletal muscle. The model has been implemented into the non-linear finite element programme LS-DYNA by means of user-defined material subroutines. There is a total of 13 parameters in the developed model and it is found that 5 of them ($b, c, \alpha, \beta$, and $A$) have been determined by best fitting to the corresponding experimental data (as performed and indicated by other authors), four of them ($\sigma_0, S, \dot{\lambda}_m^{min}$, and $\lambda_{opt}$) have their physical meanings, four of them ($\sigma_0, k_c, k_e$, and $d$) have their own value ranges and parameter $D$ is a compressibility constant. To investigate if this model can predict the experimental data by tuning the parameters within their value ranges, the experimental data from the New Zealand white rabbit hind leg muscle tibialis anterior are used and passive and activated elongations are simulated. The results show that the model is able to predict both passive and active behaviour of rabbit muscle up to 15 per cent engineering strain. The sensitivity study of some input parameters is also performed and the results can help understand how these parameters affect the total muscle stress.

Hill-type muscle models are phenomenologically based. Therefore most of the material parameters in this paper are phenomenological and few of them have direct physical counterparts. It is hoped that physically based skeletal muscle constitutive models can be proposed in the future, where all of the material parameters will be experimentally determined.

## ACKNOWLEDGEMENT

Y. T. Lu would like to thank the Engineering and Physical Sciences Research Council (EPSRC) for funding his PhD study.



## REFERENCES

1 **Hill, A. V.** The heat of shortening and the dynamic constants of muscle. *Proc. R. Soc. Lond. [Biol.]*, 1938, **126**(843), 136–195.

2 **Huxley, A. F.** Muscle structure and theories of contraction. *Prog. Biophys. Chem.*, 1957, **7**, 257–318.

3 **Audu, M. L.** and **Davy, D. T.** The influence of muscle model complexity in musculoskeletal modelling. *J. Biomed Engng*, 1985, **107**(2), 147–157.

4 **Pandy, M. G., Zajac, F. E., Sim, E.,** and **Levine, W. S.** An optimal control model for maximum-heigth human jumping. *J. Biomech.*, 1990, **23**(12), 1185–1198.

5 **Winters, J. M.** Hill-based muscle models: a systems engineering perspective. In *Multiple muscle systems: biomechanics and movement organisation* (Eds J. M. Winters and S. Y. Woo), 1990, pp. 69–96 (Springer-Verlag, New York).

6 **Zajac, F. E., Topp, E. L.,** and **Stevenson, P. J.** A dimensionless musculotendon model. In Proceedings of Eighth Annual Conference of IEEE Engineering in Medical and Biology Society, Worthington Hotel in Fort Worth, Texas, 7–10 November 1986, pp. 601–604.

7 **Johansson, T., Meier, P.,** and **Blickhan, R.** A finite element model for the mechanical analysis of skeletal muscle. *J. Theor. Biol.*, 2000, **206**(1), 131–149.

8 **Hedenstierna, S., Halldin, P.,** and **Brolin, K.** Evaluation of a combination of continuum and truss finite elements in a model of passive and active muscle tissue. *Comput. Methods Biomech. Biomed. Engng*, 2008, **11**(6), 627–639.

9 **Pato, M. P. M.** and **Areias, P.** Active and passive behaviors of soft tissues: Pelvic floor muscles. *Int. J. Numer. Meth. Biomed. Engng*, 2010, **26**(6), 667–680.

10 **Kojic, M., Mijailovic, S.,** and **Zdravkovic, N.** Modelling of muscle behavior by the finite element

method using Hill's three-element model. *Int. J. Numer. Meth. Engng*, 1998, **43**(5), 941–953.
11 **Martins, J. A. C., Pires, E. B., Salvado, R.,** and **Dinis, P. B.** A numerical model of passive and active behaviour of skeletal muscles. *Comput. Methods Appl. Mech, Engng*, 1998, **151**(3–4), 419–433.
12 **Martins, J. A. C., Pato, M. P. M.,** and **Pires, E. B.** A finite element model of skeletal muscle. *Virtual Phys. Prototyping*, 2006, **1**(3), 159–170.
13 **Tang, C. Y., Zhang, G.,** and **Tsui, C. P.** A 3D skeletal muscle model coupled with active contraction of muscle fibres and hyperelastic behavior. *J. Biomech.*, 2009, **42**(7), 865–872.
14 **Humphrey, J. D.** and **Yin, F. C.** On constitutive relations and finite deformations of passive cardiac tissue: 1. A pseudostrain-energy function. *J. Biomech. Engng*, 1987, **109**(4), 298–304.
15 **Blemker, S. S., Pinsky, P. M.,** and **Delp, S. L.** A 3D model of muscle reveals the causes of nonuniform strains in the biceps brachii. *J. Biomech.*, 2005, **38**(4), 657–665.
16 **Meier, P.** and **Blickhan, R.** FEM-simulation of skeletal muscle: the influence of inertia during activation and deactivation. In *Skeletal muscle mechanics: from mechanisms to Function* (Ed. W. Herzog), 2000, pp. 207–224 (John Wiley, New York).
17 **Fung, Y. C.** *Biomechanics: mechanical properties of living tissue,* first edition, 1981 (Springer-Verlag, New York).
18 **Belytschko, T., Liu, W. K.,** and **Moran, B.** *Nonlinear finite elements for continua and structures,* first edition, 2000 (Wiley, New York).
19 **Marsden, J. E.** and **Hughes, T. J. R.** The Mathematical Foundations of Elasticity, 1994 (Dover Publications, Inc., New York).
20 **Weiss, J. A., Maker, B. N.,** and **Govindjee, S.** Finite element implementation of incompressible, transversely isotropic hyperelasticity. *Comput. Methods Appl. Mech. Engng.*, 1996, **135**(1), 107–128.
21 *LS-DYNA keyword user's manual*, Version 971, 2007 (Livermore Software Technology Corporation, Livermore, CA, United States).
22 **Martins, J. A. C., Pato, M. P. M., Pires, E. B., Jorge, R. M., Parente, M.,** and **Mascarenhas, T.** Finite element studies of the deformation of the pelvic floor. *Ann. N. Y. Acad. Sci.*, 2007, **1101**, 316–334.
23 **Pinto, J. G.** and **Fung, Y. C.** Mechanical properties of the heart muscle in the passive state. *J. Biomech.*, 1973, **6**(6), 597–616.
24 **Chen, D. T.** and **Zelter, D.** Pump it up: Computer animation of a biomechanical based model of muscle using the finite element method. *Comput. Graph.*, 1992, **26**(2), 89–98.
25 **Zajac, F. E.** Muscle and tendon: properties, models, scaling and application to biomechanics and motor control. *Crit. Rev. Biomed. Engng*, 1989, **17**(4), 359–411.
26 **Close, R.** Dynamic properties of fast and slow skeletal muscle of the rat during development. *J. Physiol.*, 1964, **173**(1), 74–95.
27 **Otten, E.** A myocybernetic model of the jaw system of the rat. *J. Neurosci. Methods*, 1987, **21**(2–4), 287–302.
28 **Van Leeuwen, J. L.** Optimum power output and structural design of sarcomeres. *J. Theor. Biol.*, 1991, **149**(2), 229–256.
29 **Ből, M.** and **Reese, S.** Micromechanical modelling of skeletal muscles based on the finite element method. *Comput. Methods Biomech. Biomed. Engng*, 2008, **11**(5), 489–504.
30 **McMahon, T. A.** *Muscles, reflexes and locomotion*, 1984 (Princeton University Press, New Jersey).
31 **Gordon, A. M., Huxley, A. F.,** and **Julian, F. J.** The variation in isometric tension with sarcomere length in vertebrate muscle fibres. *J. Physiol.*, 1966, **184**(1), 170–192.
32 **Davis, J., Kaufman, K. R.,** and **Lieber, R. L.** Correlation between active and passive isometric force and intramuscular pressure in the isolated rabbit tibialis anterior muscle. *J. Biomech.*, 2003, **36**(4), 505–512.
33 **Myers, B., Wooley, C. T., Slotter, T. L., Garrett, W. E.,** and **Best, T. M.** The influence of strain rate on the passive and stimulated engineering stress–large strain behaviour of the rabbit tibialis anterior muscle. *J. Biomech. Engng*, 1998, **120**(1), 126–132.

## APPENDIX

### Notation

| | |
|---|---|
| $\mathbf{a}$ | deformed muscle fibre direction |
| $\mathbf{A}$ | initial muscle fibre direction |
| $b$, $c$ | material parameters in the isotropic matrix |
| $\bar{\mathbf{B}}$ | left Cauchy–Green deformation tensor with the volume change eliminated |
| $\mathbf{C}$ | right Cauchy–Green deformation tensor |
| $d$ | offset of the eccentric function |
| $D$ | compressibility constant |
| $\mathbf{E}$ | green strain |
| $f_t$ | muscle activation function |
| $f_v$ | muscle stress–velocity function |
| $f_\lambda$ | muscle stress–stretch function |
| $\mathbf{I}$ | second-order unit tensor |
| $\bar{I}_1^C$ | modified first invariant of the right Cauchy–Green strain tensor |
| $J$ | Jacobian of the deformation gradient |
| $k$ | ratio of the length of contractile element to that of series elastic element |
| $k_c$, $k_e$ | shape parameters of the hyperbolic curves |

| | |
|---|---|
| $n_1$ | muscle activation level before and after the activation |
| $n_2$ | muscle activation level during the activation |
| $S$ | exponential factor |
| $t_0$ | muscle activation time |
| $t_1$ | muscle deactivation time |
| $U$ | strain energy in the muscle |
| $U_\mathrm{f}$ | strain energy in the muscle fibres |
| $U_\mathrm{I}$ | strain energy in the isotropic matrix |
| $U_\mathrm{J}$ | strain energy associated with the volume change |
| | |
| $\alpha$, $\beta$ | material parameters in the series elastic element |
| $\bar{\lambda}_\mathrm{f}$ | fibre stretch ratio |
| $\dot{\lambda}_\mathrm{m}$ | stretch rate in the contractile element |
| $\dot{\lambda}_\mathrm{m}^\mathrm{min}$ | mimimum stretch rate |
| $\lambda_\mathrm{opt}$ | optimal fire stretch |
| $\lambda_\mathrm{s}$ | stretch ratio in the series elastic element |
| $\xi^\mathrm{CE}$ | a strain-like quantity |
| $\boldsymbol{\sigma}$ | Cauchy stress in skeletal muscle |
| $\sigma_\mathrm{c}$ | Cauchy stress produced in the contractile element |
| $\boldsymbol{\sigma}_\mathrm{fibre}$ | Cauchy stress in the muscle fibres |
| $\boldsymbol{\sigma}_\mathrm{incomp}$ | Cauchy stress related to the muscle incompressibility |
| $\boldsymbol{\sigma}_\mathrm{matrix}$ | Cauchy stress in the matrix |
| $\sigma_\mathrm{p}$ | Cauchy stress produced in the parallel element |
| $\sigma_\mathrm{s}$ | Cauchy stress produced in the series elastic element |
| $\sigma_0$ | maximum isometric stress |